

Reference value of testicular temperature measured by finite element analysis after first staged inguinal orchidopexy in children with abdominal testis and short spermatic cord

Mehdi Shirazi^{1, 2}, Ali Eslahi^{1, 3}, Mohsen Ostovari⁴, Faisal Ahmed⁵, Ahmed Zaid¹, Mohammad Reza Askarpour¹, Hossein-Ali Nikbakht⁶, Zeinab Gholami⁷, Sania Shirazi⁸

¹ Department of Urology, School of Medicine, Shiraz University of Medical Sciences, Shiraz, Iran;

² Histomorphometry and Stereology Research Center, Shiraz University of Medical Sciences, Shiraz, Iran;

³ Shiraz Geriatric Research Center, Shiraz University of Medical Sciences, Shiraz, Iran;

⁴ Department of Medical Physics and Biomedical Engineering, School of Medicine, Shiraz University of Medical Sciences, Shiraz, Iran;

⁵ Department of Urology, School of Medicine, Ibb University, Ibb, Yemen;

⁶ Social Determinants of Health Research Center, Department of Biostatistics and Epidemiology, Faculty of Medicine, Babol University of Medical Sciences, Babol, Iran;

⁷ Department of Radiology, School of Medicine, Shiraz University of Medical Sciences, Shiraz, Iran;

⁸ Student Research Committee, Shiraz University of Medical Sciences, Shiraz, Iran.

Summary

Purpose: In this study, we aimed to build a 3D reconstruction computed simulation

model and to establish a regression equation for detecting the testis's temperature by its location after first staged open orchidopexy in children with abdominal undescended testis (UDT) and short spermatic cords.

Methods: In this cross-sectional study, we enrolled 31 children with abdominal UDT and short spermatic cords who underwent first staged orchidopexy between 2017 and 2020. Using ultrasonography to obtain the testis's location distance from the skin surface (X_1), external iliac vessel (X_2), and internal inguinal ring (X_3), we input the data into a 3D reconstruction computed simulation along with COMSOL to calculate the testicular temperature. We also used multivariate regression to establish the testicular temperature regression equation from the gathered data.

Result: The mean age of the participants was 4.47 ± 1.21 years. The mean size of the operated testis was 0.39 ± 0.13 cc.

The mean distance of the testis from X_1 , X_2 , and X_3 was 3.27 ± 1.25 mm, 21.06 ± 6.42 mm, and 27.19 ± 10.09 mm, respectively. The testicular temperature regression equation derived from testis location was calculated by the formula: $34.57 + 0.0236 X_1^2 - 0.0105 X_2 - 0.0018 X_3$. The concordance for testis temperature calculated via the computational method and regression equation was 83%.

Conclusions: The current study provided a reference value for the testicular temperature of children with abdominal UDT and short spermatic cords after the first stage of orchidopexy. A testicular temperature regression equation can be established based on the testis location, which will provide relevant information for the testicular development assessment, disease diagnosis, and follow-up, and possibly determination of the time of the second stage of orchidopexy.

KEY WORDS: Abdominal testis; Temperature; Short spermatic cord; Finite element; Referential values; Simulation method.

Submitted 1 July 2023; Accepted 27 July 2023

INTRODUCTION

One of the most common birth anomalies in children is undescended testis (UDT), with estimates ranging from 1 to 4.6% of full-term newborn males affected by one or both testes failing to descend (1). Congenital UDT is caused by the failure of the first or second stage of testicular descent. Some theories about the causes of UDT include primary testicular hormonal dysfunction, secondary hormonal dysfunction (hypothalamic-pituitary axis deficiency or placental failure to produce chorionic gonadotropin), and anatomical defects in the mechanism of descent (2). Testicular maldevelopment in children with UDT is characterized by disturbed tubular structure, mainly by decreased germ cells and quantitative and qualitative changes in the Leydig cells. These tubular alterations are detectable from the UDT's first or second year of life (3). The histologic disturbances in the UDT might be related to the increased testicular exposure to elevated extra scrotal temperature (4).

Intra-abdominal testis with a short spermatic cord that does not allow the surgeons to place it in the scrotum represents approximately 30% of all UDT cases (5). There is no consensus regarding the best operation because of the testicular artery and vein length, which limits the distal placement of the testis into the scrotum. For these particular cases, the surgical solution proposed is first-stage superficial inguinal orchidopexy, then scrotal orchidopexy, two-stage laparoscopic Fowler-Stephens orchidopexy, and/or autotransplantation (6).

The testis's temperature is 2 to 4°C below the core body (6). Scrotal thermoregulation serves to liberate the large amount of heat produced during spermatogenesis. Several supporting mechanisms like thin skin with abundant vascularization, numerous sweat glands, and the absence of subcutaneous fat facilitate heat exchange and maintain the testicular temperature below body temperature (7).

In UDT patients, monitoring the testis's temperature can provide valuable information for assessing disease progression and therapeutic efficacy and might help choose optimal surgery timing. However, it is impossible to measure temperature distribution directly inside the human body to validate simulation because of ethical considerations.

Alternative approaches have been proposed to model scrotal cutaneous thermoregulation based on the automatic control theory, such as the *computed tomography-based finite element model* (CT-FEM) (8, 9). Pham *et al.* used COMSOL FEM for the thermal simulation of testis to understand the dynamics of temperature change with time and location throughout the testicle after heat was applied to the surface of the testicle (10).

Few detailed studies on the testis's temperature have been performed in the superficial inguinal region after the first stage of open orchiopexy. The anatomical heterogeneity and the diverse geometry of the testis in the superficial inguinal area make it impossible to accurately predict the testis's temperature in this location with the usual methods (11).

The present study aimed to build a 3D reconstruction computed simulation model and to establish a regression equation for detecting the testis's temperature by its location after first staged open orchidopexy in children with abdominal (UDT) and short spermatic cords.

MATERIALS AND METHODS

The Ethics Committee of Shiraz University of Medical Sciences approved the study protocol (IR.SUMS.MED.REC.1397.598) which was in accordance with the Declaration of Helsinki. Additionally, each participant's family provides written informed consent.

Study design

In this retrospective cross-sectional study, from June 2017 to June 2020, we enrolled 31 patients with previous abdominal UDT and short spermatic cord that underwent the first stage of superficial inguinal orchiopexy at least six months prior to selection in Shiraz University Hospital (Shaheed Faghihi Hospital, Ali Asghar Hospital, and Namazi Hospital).

Exclusion criteria

Patients with congenital anomalies, scrotal orchidopexy, previous orchiectomy, prior hernia surgery, or other pathological conditions affecting the development of the external genitalia were excluded.

A computational model for calculating the testis temperature

It is impossible to directly measure temperature distribution inside the human body to validate simulation due to ethical considerations. In this study, we used a computed tomography-based finite element model to estimate the temperature inside the body. This method consisted of several steps, which can be described as follows:

1. *Measuring essential and influential parameters of the testis using ultrasonography (US) imaging:* Before performing an inguinal testis ultrasound examination, adequate reassur-

ance was given. The patients were placed in a supine position and covered with a towel. Palpation was performed to assess the testis in the superficial inguinal area. A US system with high-frequency broadband linear transducer (10 MHz) and high resolution (Ws850; Samsung, Seoul, South Korea) was used to determine the structure and volume of the testis. Testis's volume was calculated using the ellipsoid formula: (volume = $0.523 \times \text{length} \times \text{thickness} \times \text{width}$). The testis's structure was assessed in grayscale with the same gain, focus, and depth settings. Measurements of the distance were taken by the testis's distance from the skin surface (X_1), external iliac vessel (X_2), and internal inguinal ring (X_3) to the testis. Table 1 shows these measurement results.

2. *Building a computational phantom:* To build the model, we used a *computed tomography* (CT) scan of a patient, and using image segmentation and image processing methods, different organs in the abdominal and inguinal areas were segmented from CT images. The entire image set consisted of 250 CT image slices, each 3 mm in slice thickness and of a matrix size of 512×512 pixels (12, 13). Then, the segmented anatomical regions were used to create a 3D model (Able Software, Lexington, MA) using Mimics Innovation Suite software toolbox. After that, the 3D model was transformed into 3-Matics software to generate a computational volumetric model.

3. *Examining the equations and heat transfer in the computer model using COMSOL software:* To solve the heat transfer equations and calculate the temperature of different parts, we converted the computational model created by 3-Matics software into executable formats in the COMSOL software (12, 14). Then, the initial processing of these models was performed to solve the heat transfer equations (15). The final model consisted of the skin surface (X_1), external iliac vessel (X_2), internal inguinal ring (X_3), and testis, and the area between them was filled with soft tissue with specific thermodynamic properties to better represent the testis environment in the patient's body (16). Also, the outside ambient temperature, abdominal cavity temperature, iliac artery temperature, and skin surface temperature in the upper scrotal region were considered based on previous studies to be 27°C , 37°C , 36.5°C , and 32°C , respectively (17). Using these constant temperature regions and solving the bio-heat equation with the finite element method in COMSOL software, the temperature of other parts inside the abdomen, testis, and soft tissue around it were calculated. For each patient, the parameters of the testis distance from the skin surface (X_1), external iliac vessel (X_2), internal inguinal ring (X_3), and testis volume were applied in a computational model. (Figure 1).

4. *Establish a regression equation:* In order to establish an equation between the parameters measured in the US imaging and the temperature calculated for the testis in a computer simulation, we sought consultation with a statistician. We were advised to use a multivariate regression statistical model (Table 1).

5. *Statistical analysis:* Statistical analysis was performed

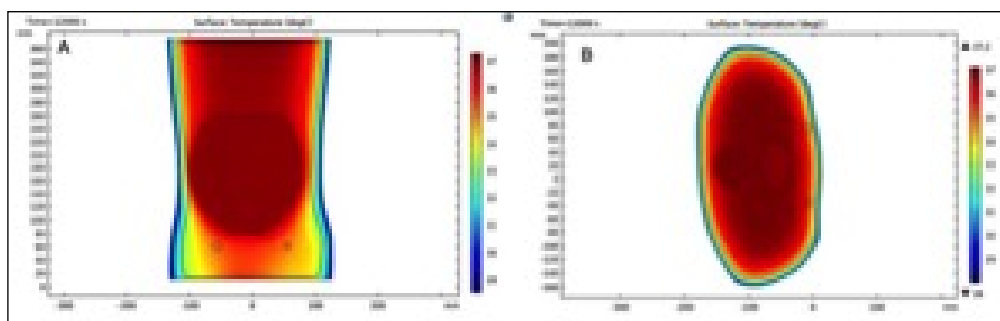


Figure 1.
(A and B): A computer model created in COMSOL software.

using SPSS (IBM SPSS, version 22, Armonk, New York: IBM Corp). Descriptive statistics for variables were calculated as mean and standard deviation. Multivariate linear regression was used to estimate the relationship between the measured variables with US (distance from skin surface, iliac vessels, and internal inguinal ring) and testis temperature calculated with computer simulation. Then, mathematical formula was represented by an equation. This analysis presented standard and non-standard regression coefficients and their 95% confidence interval.

Finally, Bland-Altman plots and Pitman’s tests were applied to compare and agree for two temperatures checked by simulation and mathematical formula assessment methods. P-values less than 0.05 were considered significant.

RESULTS

The mean age of the participants was 4.47 ± 1.21 years (range 2.5-7 years). 11 (35.5%) children had left UDT, while 20 (64.5%) children had right UDT. The mean size

Table 1.
Data of the testis volumes, temperatures, and the distance from variable locations in all the patients.

No	Distance from external Iliac vessels (mm)	Distance from internal inguinal ring (mm)	Distance from the skin surface (mm)	Testis temperature by Computer Simulation (°C)	TestisVolume (ml)	Testis temperature by fitting formula* (°C)
1	22	11	7	35.44	0.24	35.48185411
2	9	8	3	34.73	0.23	34.67952861
3	24	35	2	34.51	0.56	34.35409452
4	16	29	5	35.02	0.34	34.94528678
5	13	17	2	34.5	0.29	34.50285529
6	32	21	2.3	34.32	0.64	34.32592489
7	21	30	4.5	34.82	0.28	34.77862047
8	5	8	2.2	34.65	0.55	34.62340101
9	12	17	4	34.85	0.37	34.79679894
10	19	18	5	35.04	0.62	34.93381565
11	23	18	2.3	34.43	0.49	34.4261874
12	25	39	5.6	35.06	0.67	34.98242921
13	19	41	1.8	34.29	0.42	34.377823
14	24	19	3	34.52	0.45	34.50144957
15	17	28	3.5	34.64	0.37	34.63545896
16	22	31	2.5	34.4	0.36	34.43561217
17	25	30	2.3	34.35	0.22	34.38317657
18	18	12	4.5	34.88	0.37	34.84313672
19	16	23	3.5	34.81	0.27	34.65513524
20	30	37	2	34.33	0.42	34.28725284
21	18	28	3	34.54	0.29	34.54817069
22	25	39	1.9	34.25	0.38	34.32703646
23	19	23	4	34.35	0.34	34.71211013
24	27	35	2.3	34.3	0.73	34.35296973
25	24	28	3.8	34.43	0.39	34.61346789
26	34	39	2	34.25	0.25	34.2414723
27	18	30	3	34.53	0.31	34.5445124
28	25	34	2.9	34.42	0.35	34.4495474
29	22	39	3	34.68	0.45	34.48592786
30	30	41	3.5	34.64	0.24	34.47478277
31	19	35	4	34.41	0.25	34.69016043

*The formula is: $T(^{\circ}C) = 34.57 + 0.0236 X_1^2 - 0.0105 X_2 - 0.0018 X_3$

Table 2.
Characteristics of the patients and testis (N = 31).

Variables	Mean ± SD (Range)
Mean age (years)	4.47 ± 1.21 (2.5-7)
Mean testis size (ml)	0.39 ± 0.13 (0.22-0.73)
Mean testis temperature (°C) *	34.59 ± 0.28 (34.25-35.44)
Mean distance from the skin surface (mm)	3.27 ± 1.25 (1.8-7)
Mean distance from iliac vessels (mm)	21.06 ± 6.42 (5-34)
Mean distance from internal inguinal ring (mm)	27.19 ± 10.09 (8-41)

of the operated testis was 0.39 ± 0.13 ml (ranging from 0.22-0.73 ml). The mean distances of the testis from the skin surface, external iliac vessel, and internal inguinal ring were 3.27 ± 1.25 mm, 21.06 ± 6.42 mm, and 27.19 ± 10.09 mm, respectively. The mean testis temperature was 34.59 ± 0.28°C (ranged 34.25-35.44°C).

Table 2 demonstrates the patient and testis characteristics (Table 2).

Table 3.
The relationship between simulated testis temperature and three measurement indicators.

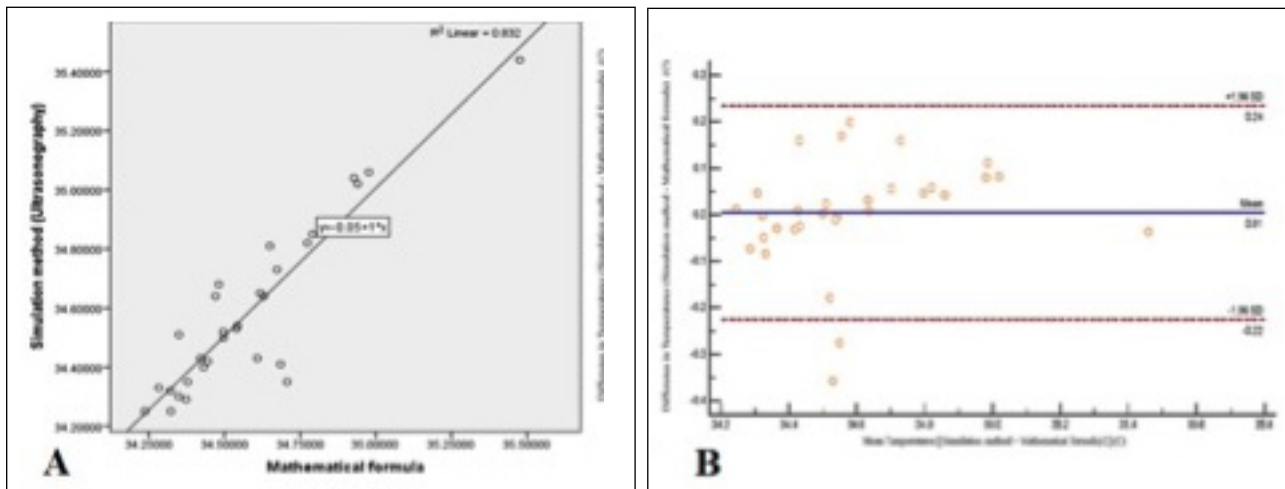
Variable	Coefficients (B)	Standard error	Beta	95% Confidence Interval		P-value
				lower	upper	
Distance from the skin (mm) ²	0.024	0.002	0.823	0.019	0.028	0.000
Distance from iliac vessels (mm)	-0.011	0.004	-0.237	-0.020	-0.001	0.026
Distance from the internal inguinal ring (mm)	-0.002	0.003	-0.065	-0.008	0.004	0.538

Multiple R = 0.912; R Square = 0.832; Adjusted R Square = 0.813.

Figure 2.

A: Scatter plots for temperatures between the simulation method and mathematical fitting formula; Pearson's correlation ($r = 0.912, p < 0.001$),

B: Bland-Altman plot for agreement of temperatures checked by the simulation method and mathematical fitting formula.



Establish a regression equation

Using multivariate regression, the testicular temperature regression equation derived from its location was calculated by the formula:

$$T = 34.57 + 0.0236 X_1^2 - 0.0105 X_2 - 0.0018 X_3 \text{ (Equation. 1)}$$

while X_1 = Distance from Skin (mm), X_2 = Distance from Iliac Vessels (mm), X_3 = Distance from the internal inguinal ring (mm), T = Temperature of testes center (°C).

Prediction of the simulation method using linear regression

The results showed that the three measured variables (distance from skin, iliac vessels, and internal inguinal ring) together predicted 83% of the testis's temperature changes, which was statistically significant (Table 3).

Also, the results showed that the distance from the skin surface variable had a robust and positive correlation with the simulated temperature of the testes. Also, the iliac vessels had a low inverse correlation with the simulated temperature, which was statistically significant. However, the internal inguinal ring had a weak inverse correlation, which was insignificant and had a minor role in prediction.

The Bland-Altman plot from Standard and Formula limits of agreement for temperatures were between -0.229 to 0.240, with a mean difference of 95% CI: 0.005 (-0.038 to 0.048) and a range of 34.24 to 35.45. The spread around the mean for temperatures shows consistent variations across all levels, and only a few participants fell

outside the limit of the agreement. The mean difference was not associated with the means of the two methods, confirming an acceptable level of agreement (Pitman's test of difference invariance: $r = 0.223, n = 31, p = 0.229$) (Figure 2).

DISCUSSION

To our knowledge, this is the first series of pediatric orchipexies reported from a single institution, and the

first to be accompanied by a finite element model for assessing the testicular temperature and establishing a regression equation by its location after open first staged superficial inguinal orchiopexy in children with abdominal UDT and short spermatic cords. Our model provides great value for the testicular development assessment, and it may be possible to decide on the time of the second stage of orchiopexy.

The thermal modeling of human tissue is important as a tool to investigate the effect of external heat sources and to predict abnormalities in the tissue. The modeling of heat transport in human tissue was first introduced by Pennes based on the heat diffusion equation (18). The equation is normally called *Pennes' bioheat equation* and is frequently used for the analysis of heat transfer in human tissues. The topic of temperature increase in human tissue after exposure to electromagnetic waves has been of interest for several years. There are some experimental studies in animals such as rats, cows, and pigs (9). However, the results may not represent the practical behavior of human tissues.

Finite element image evaluation of the scrotal surfaces is an easy and quick solution, shown to be a practical, non-invasive, and risk-free technique, as was previously shown for other species (9, 19). *Wessapan et al.* developed a 3D model of the human head to investigate the specific absorption rate and temperature distributions in the human head and testis during exposure to mobile phone radiation (9, 19). *Keangin et al.* carried out a numerical simulation of liver cancer treated using a complete mathematical model that considered the coupled model of electromagnetic wave propagation and heat transfer (20). Although many advanced transport models of biological tissue have been proposed, the minimum data requirement and easy implantation of *Pennes' bioheat model*, still make it a good approximation and a widely used model of heat transfer in biological tissues.

In this study, a case of simulated results was validated against the results with the model studied by *Kang et al.* (11). We used the computer simulation method to evaluate the testis parameters of UDT patients and the relationships of these variables with testis temperatures. According to this method, it has been reported that the counter-current heat-exchange mechanism involving the spermatic artery and the pampiniform plexus represents the primary system that controls the testis' temperature to preserve normal spermatogenesis (21). A computer-assisted model of the counter-current heat-exchange mechanism at the testicular vascular pedicle simulates the normalization of the upset heat-exchange gradient mechanism through the correction of the physical parameters and, consequently, the rheology of the blood flow in the pampiniform plexus, considering the testis as a reservoir for space-variable, time-constant heat dissipation (22).

In our study, the testis temperature was not correlated with age and testis volume. In the same manner, *Mieusset et al.* reported that the testis temperature was not associated with age, empty intra-scrotal cavity, and the simultaneous rectal temperature (3). *Kenneth et al.* measured the intratesticular and scrotal skin temperatures in 34 men who had undergone scrotal or inguinal surgical procedures. Scrotal temperatures were measured before and

after a dry scrotal shave. The intratesticular temperature was measured under direct vision with a needle thermistor, revealing a strong correlation between the intratesticular and scrotal skin temperatures. These observations suggest that scrotal skin temperature measurements might help detect elevations of intratesticular temperature (23). Similarly, our result showed that the distance from the external iliac vessel and skin surface had a more significant effect on the testis temperature ($p = 0.0012, 0.0037$), respectively. The positive correlation between the testis temperature and distance from the skin surface and the external iliac vessel reveals the interdependence between the scrotum areas in the testis thermoregulation, which was in line with the result of *Ruediger et al.* study (24).

In our study, the correlation between the temperatures of the testis and the distance from the internal inguinal ring was less significant in comparison to other parameters that affect the testis temperature ($p = 0.1943$). This poor correlation can be explained by a lesser heat exchange area. According to *Kastelic et al.*, the ambient temperature had a significant effect on the temperature of the lower region of the scrotum, a negligible impact on the temperature of the upper region, and an intermediate effect on the temperature of the middle region of the scrotum (25). The dominant process in the heat energy transfer between the testis and their surroundings is the heat conduction process. The following equation expresses the rate of heat transfer:

$$\frac{\Delta Q}{\Delta t} = -kA\nabla T \quad (\text{Equation. 2})$$

K is the conductivity coefficient, A is the contact cross-section, and is the temperature gradient. The negative sign in this formula indicates that heat transfers from the higher temperature region to the lower temperature region. The temperature gradient (∇T) is defined as the temperature ratio of two environmental points to their spatial distance (26, 27). Since, in UDT patients, heat transfer through the testis and temperature reduction is disrupted, we aim to find the location that provides better heat emission to cool down the testis.

In the abdomen, heat sources are the main arteries and the body's core region in the thermoregulation system that have a temperature higher than that of the testicles, and the heat sink area is the skin surface through which heat energy is transferred out of the body.

During UDT surgery, it is impossible to change such parameters as thermal conductivity (k) and the cross-sectional area of the testis and the surrounding tissues (A), whereas the location of the testis is the only parameter that the surgeon can adjust. The surgeon can control the temperature gradient by changing the distance between the testicles and the heat sources or the heat sinks. There is a temperature gradient between the testis and the three areas of the internal inguinal ring, external iliac vessel, and skin surface. The temperature of the external iliac vessel and the internal inguinal ring are equal to the core body temperature and higher than the temperature of the testis, but the temperature of the skin surface is close to the ambient temperature and is lower than that of the testis (6).

The results of this study show that among the three

parameters of distance from the skin surface (X_1), distance from the iliac vessel (X_2), and distance from the internal inguinal ring (X_3), the X_1 parameter has more influence on the testicular temperature than others. In equation 1, the coefficient of X_1 is positive, so when the distance from the skin decreases, the central temperature of the testis decreases. Therefore, the most suitable position to place the testicles is the closest distance from the skin. Equation 1 also shows that between X_2 and X_3 , the influence of the X_2 on the testis temperature is more dominant than X_3 . The coefficients of X_2 and X_3 are negative. Therefore, the proper position is the one that is farthest from the iliac arteries and internal inguinal ring.

This study had several limitations, such as its retrospective nature, the lack of a control group, and the small sample size. Also, the testis size before surgery and contralateral intra-scrotal testis temperatures in children were not checked. We detected the heterogeneity of the testis size and age among the patients. The period between surgery and temperature checking was six months at least.

Therefore, this is just an observational report requiring validation with a large sample size and randomized criteria. Because the thermal factors involved in the heat exchange of children's environment are not all determinable, these models are valuable only when the children's thermal conditions and environment are both known or may be controlled.

CONCLUSIONS

The current study provided a reference value for the testicular temperature of boys with abdominal UDT and short spermatic cords after the first stage of orchiopexy. A testicular temperature regression equation derived from its location can be established, which will provide relevant information for the testicular development assessment, disease diagnosis, and follow-up, and possibly for deciding on the time of the second stage of orchiopexy.

ACKNOWLEDGMENTS

The authors would like to thank Shiraz University of Medical Sciences, Shiraz, Iran, the Center for Development of Clinical Research of Nemazee Hospital, and Dr. Nasrin Shokrpour for editorial assistance.

REFERENCES

1. Kurz D. *Current Management of Undescended Testes*. *Curr Treat Options Pediatr*. 2016; 2:43-51.
2. Hutson JM, Li R, Southwell BR, et al. *Germ cell development in the postnatal testis: the key to prevent malignancy in cryptorchidism?* *Front Endocrinol (Lausanne)*. 2012; 3:176.
3. Mieuisset R, Fouda PJ, Vaysse P, et al. *Increase in testicular temperature in case of cryptorchidism in boys*. *Fertil Steril*. 1993; 59:1319-21.
4. Humphrey G, Najmaldin A, Thomas D. *Laparoscopy in the management of the impalpable undescended testis*. *Br J Surg*. 1998; 85:983-5.

5. Wang CY, Wang Y, Chen XH, et al. *Efficacy of single-stage and two-stage Fowler-Stephens laparoscopic orchidopexy in the treatment of intraabdominal high testis*. *Asian J Surg*. 2017; 40:490-4.
6. Shiraishi K, Takihara H, Matsuyama H. *Testicular Temperature and the Effects of Orchiopexy in Infants with Cryptorchidism*. *J Urol*. 2021; 206:1031-7.
7. Ismail E, Orlando G, Pompa P, et al. *Time-domain analysis of scrotal thermoregulatory impairment in varicocele*. *Front Physiol*. 2014; 5:342.
8. Imai K. *Computed tomography-based finite element analysis to assess fracture risk and osteoporosis treatment*. *World J Exp Med*. 2015; 5:182-7.
9. Wessapan T, Rattanadecho P. *Temperature induced in the testicular and related tissues due to electromagnetic fields exposure at 900 MHz and 1800 MHz*. *Int J Heat Mass Transf*. 2016; 102:1130-40.
10. Pham S, Schultz JS. *Testicular thermoregulation with respect to spermatogenesis and contraception*. *J Therm Biol*. 2021; 99:102954.
11. Kang Z, Wang F, Udayraj. *An advanced three-dimensional thermoregulation model of the human body: Development and validation*. *Int Commun Heat Mass Transf*. 2019; 107:34-43.
12. Gür Y. *Additive Manufacturing of Anatomical Models from Computed Tomography Scan Data*. *Mol Cell Biomech*. 2014; 11:249-58.
13. Zukowska M, Rad MA, Górski F. *Additive Manufacturing of 3D Anatomical Models-Review of Processes, Materials and Applications*. *Materials (Basel)*. 2023; 16:880.
14. Sander IM, McGoldrick MT, Helms MN, et al. *Three-dimensional printing of X-ray computed tomography datasets with multiple materials using open-source data processing*. *Anat Sci Educ*. 2017; 10:383-91.
15. Steinberger A. *Effects of Temperature on the Biochemistry of the Testis*. In: Zorngniotti AW, editor. *Temperature and Environmental Effects on the Testis*. Boston, MA: Springer US; 1991. p. 33-47.
16. Popovic M, Pantovic Pavlovic M, Pavlovic M. *Ghosts of the past: Elemental composition, biosynthesis reactions and thermodynamic properties of Zeta P.2, Eta B.1.525, Theta P.3, Kappa B.1.617.1, Iota B.1.526, Lambda C.37 and Mu B.1.621 variants of SARS-CoV-2*. *Microb Risk Anal*. 2023; 24:100263.
17. Taylor NA, Tipton MJ, Kenny GP. *Considerations for the measurement of core, skin and mean body temperatures*. *J Therm Biol*. 2014; 46:72-101.
18. Pennes HH. *Analysis of tissue and arterial blood temperatures in the resting human forearm*. 1948. *J Appl Physiol (1985)*. 1998; 85:5-34.
19. Siriwitpreecha A, Rattanadecho P, Wessapan T. *The influence of wave propagation mode on specific absorption rate and heat transfer in human body exposed to electromagnetic wave*. *Int J Heat Mass Transf*. 2013; 65:423-34.
20. Keangin P, Rattanadecho P, Wessapan T. *An analysis of heat transfer in liver tissue during microwave ablation using single and double slot antenna*. *Int J Heat Mass Transf*. 2011; 38:757-66.
21. Sheehan MM, Ramasamy R, Lamb DJ. *Molecular mechanisms involved in varicocele-associated infertility*. *J Assist Reprod Genet*. 2014; 31:521-6.
22. Tritto G. *Computer-assisted simulation model of the counter-current heat-exchange mechanism at the testicular vascular pedicle*. *Proceedings of the Annual International Conference of the IEEE Engineering in Medicine and Biology Society*; 1988 4-7 Nov. 1988.

23. Kurz KR, Goldstein M. Scrotal temperature reflects intratesticular temperature and is lowered by shaving. *J Urol.* 1986; 135:290-2.
24. De Ruediger FR, Chacur MGM, Alves FCPE, et al. Digital infrared thermography of the scrotum, semen quality, serum testosterone levels in Nellore bulls (*Bos taurus indicus*) and their correlation with climatic factors. *J Semina: Ciências Agrárias.* 2016; 37:221-32.
25. Kastelic J, Cook R, Coulter G, et al. Environmental factors affecting measurement of bovine scrotal surface temperature with infrared thermography. *Anim Reprod Sci* 1996; 41:153-9.
26. Kaviany M. *Heat Transfer Physics.* 2 ed. Cambridge: Cambridge University Press; 2014.
27. Lienhard JH, Lienhard JH. *A Heat Transfer Textbook.* 4th edition. ed. Newburyport: Dover Publications; 2013.

Correspondence

Mehdi Shirazi

shirazim@sums.ac.ir

Ali Eslahi

alieslahi@yahoo.com

Dpt of Urology, School of Medicine, Shiraz University of Medical Sciences, Shiraz, Iran

Faisal Ahmed

fmaaa2006@yahoo.com

Mohsen Ostovari

Mohsen.Ostovari@gmail.com

Ahmed Zaid

ahmadzaid333@gmail.com

Mohammad Reza Askarpour

askarvip2@gmail.com

Hossein-Ali Nikbakht

Ep.nikbakht@gmail.com

Zeinab Gholami

Gholamii.zb@gmail.com

Sania Shirazi

saniashirazi046@gmail.com

Conflict of interest: The authors declare no potential conflict of interest.